



CHORUS

This is the accepted manuscript made available via CHORUS. The article has been published as:

Spin Mode Switching at the Edge of a Quantum Hall System

Udit Khanna, Ganpathy Murthy, Sumathi Rao, and Yuval Gefen

Phys. Rev. Lett. **119**, 186804 — Published 2 November 2017

DOI: [10.1103/PhysRevLett.119.186804](https://doi.org/10.1103/PhysRevLett.119.186804)

Spin Mode-Switching at the Edge of a Quantum Hall System

Udit Khanna,^{1,2} Ganpathy Murthy,³ Sumathi Rao,^{1,2} and Yuval Gefen⁴

¹*Harish-Chandra Research Institute, Chhatnag Road, Jhansi, Allahabad 211019, India*

²*Homi Bhabha National Institute, Training School Complex, Anushaktinagar, Mumbai, Maharashtra 400085, India*

³*Department of Physics and Astronomy, University of Kentucky, Lexington KY 40506-0055, USA*

⁴*Department of Condensed Matter Physics, Weizmann Institute, 76100 Rehovot, Israel*

Quantum Hall states can be characterized by their chiral edge modes. Upon softening the edge potential, the edge has long been known to undergo spontaneous reconstruction driven by charging effects. In this paper we demonstrate a qualitatively distinct phenomenon driven by exchange effects, in which the *ordering* of the edge modes at $\nu = 3$ switches abruptly as the edge potential is made softer, while the ordering in the bulk remains intact. We demonstrate that this phenomenon is robust, and has many verifiable experimental signatures in transport.

PACS numbers: 73.21.-b, 73.22.Gk, 73.43.Lp, 72.80.Vp

Shortly after the discovery of the integer quantum Hall effect (QHE) it was realized that the edges of an incompressible electron gas play a crucial role in transport [1]. In a quantum Hall state, the bulk has a charge gap. Near a sharp edge, gapless chiral modes [2] carry the current between the contacts, consistent with the topologically protected transport observables of the QHE.

In the early 90s it was realized that both integer [3–5] and fractional [6, 7] edges reconstruct as the slope of the edge confining potential $V_{\text{edge}}(y)$ is made smoother. Reconstruction is the modification of the position and/or the number and nature of the edge modes [3–9]. Subsequently, various manifestations of edge reconstruction have been observed in the QHE regime [10–14], and theoretically studied in many QHE states [15–20] and in time reversal invariant topological insulators [21].

Edge reconstruction is driven by charge effects [22], as seen by the work of Dempsey *et al.* [4] who studied the unpolarized filling factor $\nu = 2$. For a sharp edge, the $n = (0\uparrow)$ and the $n = (0\downarrow)$ single-particle levels cross the chemical potential μ at the same location, with a sharp change in electron density there. As $V_{\text{edge}}(y)$ is made smoother, the \uparrow and \downarrow crossing points spontaneously move away from each other, making the density variation smoother at the edge.

In this work we focus on the edge of a $\nu = 3$ quantum Hall state and uncover edge phenomena driven by spin exchange rather than charge effects [22]. The bulk remains inert at the parameters we consider and only the edge shows a phase transition. We find that, depending on parameters, the order of the two inner or the two outer edge channels switches as $V_{\text{edge}}(y)$ becomes smoother. No charge reconstruction is observed in the regime where *spin-mode-switching* occurs. Our analysis indicates that the phase transitions are first-order. In designed geometries with controlled edge steepness and quantum point contacts (QPCs), a host of phenomena can serve as “smoking gun” tests of spin-mode-switching. These include a change in the nature of the spin trans-

port through a single QPC system with and without spin-mode-switching, and a qualitative change in the way disorder affects transport following a spin-mode-switching transition.

To set the stage for our model, we define the cyclotron energy $\hbar\omega_c = \frac{\hbar eB}{m_b}$ (m_b is the band mass), the interaction scale $E_c = \hbar\omega_c \bar{E}_c = \frac{e^2}{4\pi\epsilon\ell}$ where ϵ includes the dielectric constant of the medium, and $\ell = \sqrt{\hbar/eB}$, the magnetic length. We will work at tiny Zeeman coupling $E_z \ll E_c$.

In the Landau gauge $eA_x = -\frac{y}{\ell}$, $eA_y = 0$, the single-particle wavefunctions of the n^{th} Landau level (LL) in a system with periodic boundary conditions in x can be written as [23]

$$\Phi_{nk}(x, y) = \frac{e^{ikx} e^{-\frac{(y-k\ell)^2}{2\ell^2}}}{\sqrt{2^n n! L_x \ell \sqrt{\pi}}} H_n\left(\frac{y - k\ell}{\ell}\right), \quad (1)$$

where $k = 2\pi m/L_x$ determines the position of the guiding center along the y -axis. The Hamiltonian of the system $H = H_b + H_{e\text{-bg}}$ can be split into a electronic bulk part H_b and the electron-background interaction $H_{e\text{-bg}}$ responsible for the confining potential V_{edge} at the edge. The bulk Hamiltonian is

$$H_b = \hbar\omega_c \sum_{nks} n c_{nks}^\dagger c_{nks} + \frac{1}{2L_x L_y} \sum_{\vec{q}} v(q) : \rho_e(\vec{q}) \rho_e(-\vec{q}) : \quad (2)$$

where the electron density operator $\rho_e(x, y) = \sum_s \Psi_s^\dagger(x, y) \Psi_s(x, y)$, $\Psi_s(x, y) = \sum_{n,k} \Phi_{nk}(x, y) c_{nks}$, with c_{nks} being canonical fermion operators, and $v(q)$ and $\rho_e(\vec{q})$ are the Fourier transforms of the interaction $v(\vec{r} - \vec{r}')$ and $\rho_e(x, y)$. The possible translation-invariant ground states of the $\nu = 3$ bulk are $|\psi_1\rangle = |0\uparrow, 0\downarrow, 1\uparrow\rangle$ (partially polarized) and $|\psi_2\rangle = |0\uparrow, 1\uparrow, 2\uparrow\rangle$ (fully polarized), where we only write the occupied spin-labelled LLs. As \bar{E}_c increases there is a bulk first-order transition [24–26] driven by exchange from $|\psi_1\rangle$ to $|\psi_2\rangle$. In the Hartree-Fock (HF) approximation this occurs at $\bar{E}_c \approx 2.5$ for the Coulomb interaction.

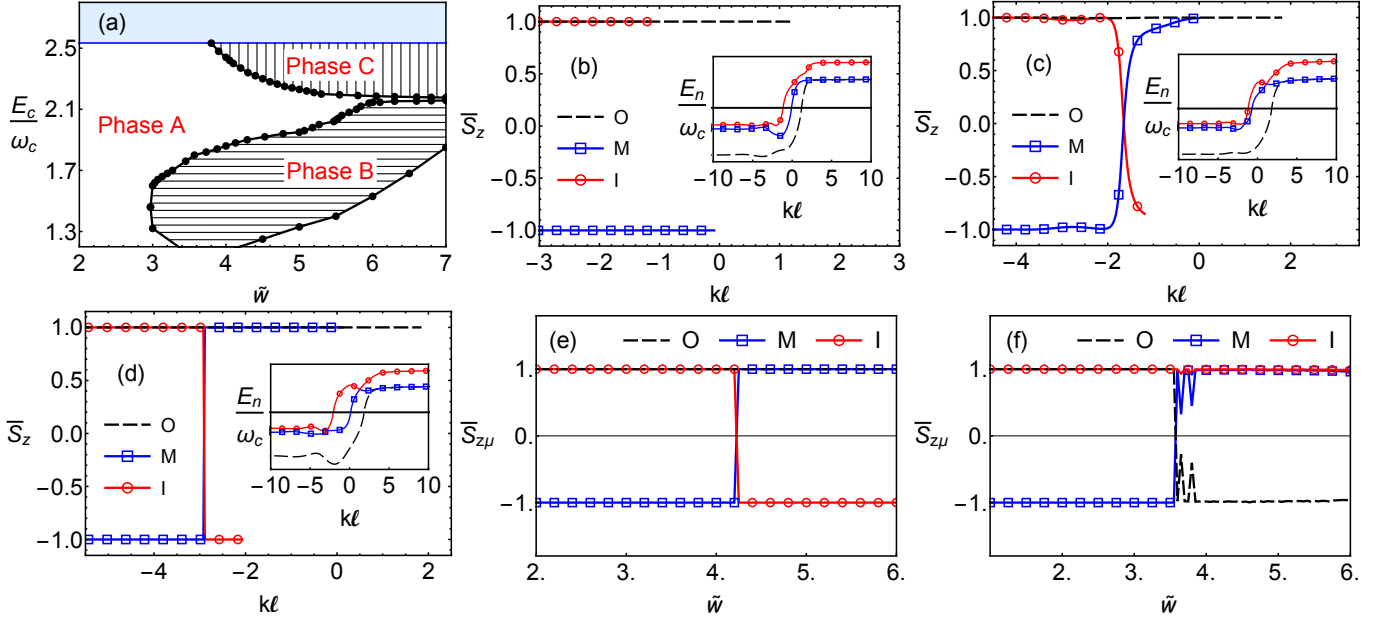


FIG. 1. (Color online) (a) The phase diagram. The background color represents the bulk phase, white being partially polarized ($|0\uparrow, 0\downarrow, 1\uparrow\rangle$) and blue being fully polarized ($|0\uparrow, 1\uparrow, 2\uparrow\rangle$). States are labelled $i = O$ (outermost), M (middle) and I (innermost). The plain white region also denotes edge Phase A ($O=0\uparrow$, $M=0\downarrow$ and $I=1\uparrow$). Edge Phase B ($O=0\downarrow$, $M=0\uparrow$ and $I=1\uparrow$) is horizontally hatched, while Phase C ($O=0\uparrow$, $M=1\uparrow$ and $I=0\downarrow$) is vertically hatched. Due to poor convergence of the HF, for $6 \leq \tilde{w} \leq 7$, $\tilde{E}_c \simeq 2.13$ it is not clear whether there is a direct transition between Phases B and C, or whether Phase A intervenes. In Figs. 1(b), 1(c) and 1(d) we depict $\bar{S}_z(i, k)$ of the occupied single-particle states versus $k\ell$ at $\tilde{E}_c = 2.3$. Only occupied levels are depicted. The line for level i terminates where the level i crosses μ , with $\bar{S}_z(i, k)$ at the μ -crossing defined as $\bar{S}_{z\mu}(i)$. The insets depict the energy dispersions of the HF single-particle states vs. $k\ell$, with the horizontal black line being μ . In Fig. 1(b) we are in Phase A ($\tilde{w} = 2.0$) where no spin rotations occur. Fig. 1(c) shows $\bar{S}_z(i, k)$ vs. $k\ell$ at the transition ($\tilde{w} = 4.28$), with spin rotations occurring over a scale ℓ , where the corresponding energy level dispersions come close together in an avoided crossing (inset). Fig. 1(d) shows $\bar{S}_z(i, k)$ vs. $k\ell$ in Phase C ($\tilde{w} = 5.0$). The spin rotations are quite abrupt, and occur where the corresponding dispersions undergo a sharp avoided crossing. In Fig. 1(e) we plot $\bar{S}_{z\mu}(i)$ vs. \tilde{w} at $\tilde{E}_c = 2.3$. A discontinuous change in $\bar{S}_{z\mu}$ for the M and I levels is seen at the transition between Phases A and C. Similar results hold at $\tilde{E}_c = 1.8$ for the Phase A to Phase B transition, with $\bar{S}_{z\mu}$ showing a discontinuous change for the O and M levels, as shown in Fig. 1(f).

The electron-background interaction is

$$H_{e\text{-bg}} = \int d^2r V_{\text{edge}}(y) \rho_e(x, y) \quad (3)$$

where $V_{\text{edge}}(y) = -\int d^2r' \rho_b(y') v(\vec{r} - \vec{r}')$ is the edge confining potential and $\rho_b(y)$ is the positive background density. In our model the background density decreases linearly to zero over a distance W at the edge [5]. The dimensionless parameter $\tilde{w} = W/\ell$ characterizes the slope of V_{edge} ,

$$\rho_b(y) = \begin{cases} \rho_0 & y < -\frac{W}{2} \\ \rho_0 \frac{\frac{W}{2} - y}{W} & -\frac{W}{2} < y < \frac{W}{2} \\ 0 & y > \frac{W}{2} \end{cases}. \quad (4)$$

Theoretical Analysis: Our primary tool is the spin-unrestricted Hartree-Fock (HF) approximation keeping up to 6 spin resolved LLs to include the effect of LL-mixing and spin-mixing. In the HF approximation, the many-body state is replaced by a variational Slater determinant, characterized by all possible averages $\langle c_i^\dagger c_j \rangle$.

We confine ourselves to translation invariant states, described by $\langle c_{nks}^\dagger c_{n'k's'} \rangle = \delta_{kk'} \Delta_{ns, n's'}(k)$. In the bulk the matrix $\Delta_{ns, n's'}$ is independent of k and diagonal in n as well as in s (no LL-mixing or spin-mixing). Near the edge $\Delta_{ns, n's'}$ acquires a k -dependence, and LL-mixing/spin-mixing will occur. The optimal Slater determinant that minimizes the variational energy is found by an iterative procedure carried out to self-consistency. At each step, an effective one-body Hamiltonian (dependent on $\Delta_{ns, n's'}(k)$) is solved and the energy levels filled up to a chemical potential chosen to satisfy overall charge neutrality. The new state enables the computation of a new set of Δ , giving the seed for the next iterative step [27]. The results of the HF calculation are shown in Fig. 1. We use a screened Coulomb interaction of the form $v(\vec{q}) = \frac{2\pi E_c}{q + q_{sc}}$, where q_{sc} is the inverse screening length. The results shown are for $q_{sc}\ell = 10^{-2}$, though spin-mode-switching persists at least up to $q_{sc}\ell = 0.5$. In unrestricted HF single-particle levels generically cannot be labelled by spin and cannot cross due to level repulsion. We therefore label the edge modes by their location

as $i = \text{O}(\text{outermost}), \text{M}(\text{middle})$ and $\text{I}(\text{innermost})$. To proceed further, we compute the quantum expectation value $\bar{S}_z(i, k)$ for each occupied single-particle state i at position kl . The spin character of the chiral edge modes transporting current are determined by the $\bar{S}_z(i, k)$ of the corresponding single-particle levels at the crossing with the chemical potential, $\bar{S}_{z\mu}(i)$. This allows us to label an edge mode with a spin.

Fig. 1(a) shows two edge-mode-switched phases. For $\tilde{w} \lesssim 3$, there is no spin-mixing, and the edges follow the bulk order: $\text{O}=0\uparrow, \text{M}=0\downarrow$ and $\text{I}=1\uparrow$. This is Phase A. For $1.5 \lesssim \tilde{E}_c \lesssim 2.13$ and $\tilde{w} > 3$, the system enters Phase B where the order of the edge modes is $\text{O}=0\downarrow, \text{M}=0\uparrow$ and $\text{I}=1\uparrow$. Phase C occurs for $2.13 < \tilde{E}_c < 2.5$ and $\tilde{w} > 3.5$, with the edge mode ordering $\text{O}=0\uparrow, \text{M}=1\uparrow$ and $\text{I}=0\downarrow$. For $6 \leq \tilde{w} \leq 7$, $\tilde{E}_c \simeq 2.13$ HF converges poorly, making it unclear whether there is a direct transition between Phases B and C, or whether a sliver of Phase A persists between them. Fig. 1(b) shows \bar{S}_z vs. kl of the three occupied levels near the edge at $\tilde{E}_c = 2.3$, $\tilde{w} = 2.0$ (Phase A). The lines terminate where the corresponding level crosses μ . Fig. 1(b) inset shows the energy dispersions of the self-consistent HF states for the same parameters. Fig. 1(c) shows \bar{S}_z vs. kl at the $A \rightarrow C$ transition ($\tilde{w} = 4.28$), and Fig. 1(d) shows the same in Phase C ($\tilde{w} = 5.0$). Figs. 1(e), 1(f) show the expectation value $\bar{S}_{z\mu}$ of the respective levels of O, M and I that intersect the Fermi energy as a function of \tilde{w} at $\tilde{E}_c = 1.8$ and 2.3. The spin characters of O, M and I show dis-

continuous jumps, which indicate 1st-order transitions in our approximation. The electron charge density hardly varies through the entire regime [22, 27].

The emergence of mode-switching is quite robust and is qualitatively unaffected by including LL/spin mixing to higher LLs ($n > 2$). Phases B and C occur over a very broad range of \tilde{w} , (Phase C exists at least up to $\tilde{w} = 11$). Upon increasing the Zeeman coupling, the bulk phase boundary between the partially and fully polarized states moves lower in \tilde{E}_c and Phase C encroaches on Phase B. Furthermore, the lower boundary between Phase A and Phase B in Fig. 1(a) moves upwards. Reducing the range of the interaction by increasing $q_{sc}\ell$ moves the phase boundaries of edge phases B and C towards larger \tilde{w} . Upon independently varying the strength of the direct (E_{cd}) and exchange (E_{cx}) terms, we find that mode-switching occurs in HF only if $E_{cx} > 0.6E_{cd}$, consistent with our claim that this is an exchange effect [22].

To get beyond the HF limitation of single particle occupation being restricted to either 0 or 1 (at $T = 0$), we investigated a class of variational states that do not conserve particle number and allow continuously varying $0 \leq n(k) \leq 1$. The simplest such state for the $\nu = 1$ spin-polarized edge is $|\psi\rangle = \prod_{k=1}^{N_s} (u_k + v_k e^{i\theta_k} c_k^\dagger)|0\rangle$. Here u_k, v_k ($u_k^2 + v_k^2 = 1$) are real numbers, and θ_k is a set of phases chosen to minimize the translation-symmetry-breaking inherent in such states. This class includes HF states. For $\nu = 3$ our variational state is [27]

$$|\psi\rangle = \prod_k (U_k + V_{0k} e^{i\theta_{0k}} c_{0k\uparrow}^\dagger + V_{1k} e^{i\theta_{1k}} c_{0k\downarrow}^\dagger c_{0k\uparrow}^\dagger + V_{2k} e^{i\theta_{2k}} c_{1k\uparrow}^\dagger c_{0k\uparrow}^\dagger + V_{3k} e^{i\theta_{3k}} c_{1k\uparrow}^\dagger c_{0k\downarrow}^\dagger c_{0k\uparrow}^\dagger)|0\rangle. \quad (5)$$

When $E_{cx} < 0.4E_{cd}$ this ansatz does produce smoothly varying $n(k)$ at $\nu = 3$, with the variational energy lower than the HF energy. However, upon increasing E_{cx} we recover the HF solution, lending further support to the validity of HF results and the transition being 1st order.

Experimental signatures. Before presenting transport signatures of mode-switching [27], we note that whenever an edge changes from sharp to smooth, spin-mixed edge modes will undergo avoided crossings with attendant spin rotations along the edge [28–30]. Further, the $\nu = 2$ state becomes fully polarized at $\tilde{E}_c \approx 2.13$ (in HF at $q_{sc} = 0$). If a QPC is tuned to be at dimensionless two-terminal conductance $g_2 = 2$, the QPC region will be fully polarized in the regime where Phase C occurs, and unpolarized in the regime where Phase B occurs.

Our first “smoking gun” signature is in spin transport, as illustrated in Fig. 2. The system is tuned to be in the $g_2 = 1$ or $g_2 = 2$ conductance plateau, with the source on the top left. Solid (dashed) lines indicate spin up

(down) modes at the edge and spin rotations in space are indicated by black circles on the figures. The current is carried by the channels O and M (Fig. 2(a)). For all edges sharp and $\tilde{E}_c > 2.13$, there is a nontrivial spin rotation of M as it enters the QPC region, but it rotates back upon exiting the QPC, so that the current in the drain (top right) remains unpolarized. When the right side is in Phase C (Fig. 2(c)), the current in the drain is spin polarized \uparrow . In Fig. 2(b) we show a QPC tuned to $g_2 = 1$ in the regime where Phase B occurs ($\text{O}=0\downarrow, \text{M}=0\uparrow$ and $\text{I}=1\uparrow$). Now the source current (top left) is \uparrow but the drain current (top right) is \downarrow .

For our next signature, we consider the effect of static, non-magnetic disorder, which allows tunneling between neighboring chiral modes of the same spin. In Fig. 2(d) and 2(e), the region outside the two QPCs is in Phase A. We tune the system to the $g_2 = 1$ plateau. If the inter-QPC region is in Phase A, the opposite spin polarizations of the two outer channels $0\uparrow, 0\downarrow$ prevent disorder-induced

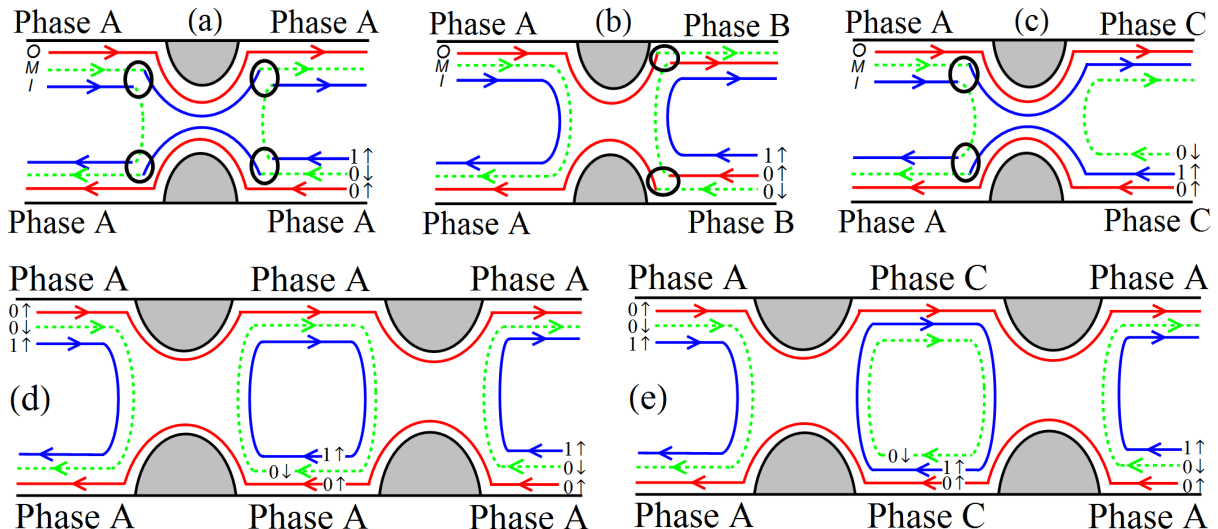


FIG. 2. (Color online) Experimental setups to show “smoking gun” signatures of mode switching. The source (drain) is always on the top left (right). Red solid lines depict the $0\uparrow$ mode, green dashed lines the $0\downarrow$ mode and blue solid lines the $1\uparrow$ mode. The edges are labelled on the bottom right of each panel. Spin rotations in space are indicated by black circles.

(a),(b) and (c) Single QPC setups. (a) All the edges are in Phase A, $g_2 = 2$, and $\tilde{E}_c > 2.13$. The full polarization of the $\nu = 2$ QPC region forces the M and I modes undergo a spin-rotation upon entering the QPC, and an inverse rotation upon exit. The incoming/outgoing current is spin unpolarized. (b) When the edges to the right of the QPC are in Phase B, the current at $g_2 = 1$ reverses spin-polarization from \uparrow to \downarrow at the QPC. (c) When the edges to the right of the QPC are in Phase C, the current (from A to C) at $g_2 = 2$ changes from spin-unpolarized to spin-polarized at the QPC.

(d) and (e) Two-QPC setups at $g_2 = 1$. (d) When the confining potential in the middle section is sharp on both the upper and lower edges (in Phase A), a high quality $g_2 = 1$ plateau emerges. (e) When the confining potential in the middle section is smooth at both edges (in Phase C), disorder-induced degradation of the conductance plateau due to backscattering in the inter-QPC region is expected.

tunneling, as shown in Fig. 2(d). If, however the inter-QPC region is in Phase C (Fig. 2(e)), the two outer channels have same spin and disorder-induced tunneling is allowed on both the top and bottom edges. This leads to backscattering, and hence to a degradation of the quantization of the conductance plateau. Similar results hold for $g_2 = 2$ when comparing setups with inter-QPC region being in Phase A or in Phase B [27].

Summary and discussion. We have found spin-exchange driven edge phases and quantum phase transitions that take place at $\nu = 3$ for low Zeeman energies. Our control parameters are the interaction strength \tilde{E}_c and the edge width \tilde{w} . We focus on $\tilde{E}_c \lesssim 2.5$: a partially polarized bulk state with the LLs $0\uparrow$, $0\downarrow$ and $1\uparrow$ occupied. For small \tilde{w} , the order of the edges follows the bulk order (Phase A). However, as \tilde{w} becomes larger, we find two distinct edge mode-switched phases: For $1.5 \lesssim \tilde{E}_c \lesssim 2.13$, Phase B occurs with the edge ordering O=outermost= $0\downarrow$, M=middle= $0\uparrow$ and I=innermost= $1\uparrow$. For $2.13 \lesssim \tilde{E}_c \lesssim 2.5$ Phase C occurs with the edge ordering O= $0\uparrow$, M= $1\uparrow$ and I= $0\downarrow$. Heuristically, these phases result from an exchange attraction between the like-spin edge modes. Employing approximate analytical methods (the spin unrestricted Hartree-Fock approximation, and minimization with respect to a particle non-

conserving variational state) we find the transitions to be 1^{st} -order. We stress that there is no significant charge rearrangement associated with these transitions, putting spin-mode-switching in a qualitatively different category from the extensively investigated phenomena of charge-driven edge reconstruction. The crucial requirements for the switching transition to occur are: (i) A partially polarized bulk state. (ii) Moderate to strong interaction strength \tilde{E}_c . (iii) A smooth edge. We have also provided (spin and charge) transport signatures of such transitions, relying on experimentally accessible setups.

Our findings have diverse implications, e.g.: (i) Bulk $\nu = 1$ supports charged skyrmions [31], while bulk $\nu = 3$ does not [32, 33]. The $\nu = 1$ spinful edge is known to be unstable to the formation of edge skyrmions [34]. Similar edge spin texture instabilities would likely arise in our $\nu = 3$ system, especially in Phase C, with some similarities to charge-neutral bilayer graphene [35]. (ii) Our results should have direct analogues at $\nu = 4$, and more interestingly, in the QHE in graphene [36–38]. (iii) Our analysis should generalize to fractional quantum Hall states such as $\nu = \frac{3}{7}$, which is the composite fermion analog [39] of the $\nu = 3$ state.

GM thanks Sid Parameswaran for illuminating discussions, and acknowledges the Aspen Center for Physics

(NSF Grant No. 1066293) for its hospitality, the US-Israel BSF (grants 2012120 and 2016130) and NSF-DMR 1306897 for support. YG thanks Dmitry G. Polyakov for useful discussions, and acknowledges ISF (grant 1349/14), the DFG (grants RO 2247/8-1, CRC 183), the IMOS Israel-Russia program, and Minerva for support.

-
- [1] B. I. Halperin, Phys. Rev. B **25**, 2185 (1982).
 [2] X.-G. Wen, Phys. Rev. Lett. **64**, 2206 (1990).
 [3] D. B. Chklovskii, B. I. Shklovskii, and L. I. Glazman, Phys. Rev. B **46**, 4026 (1992).
 [4] J. Dempsey, B. Y. Gelfand, and B. I. Halperin, Phys. Rev. Lett. **70**, 3639 (1993).
 [5] C. de C. Chamon and X.-G. Wen, Phys. Rev. B **49**, 8227 (1994).
 [6] A. H. MacDonald, Phys. Rev. Lett. **64**, 220 (1990); M. D. Johnson and A. H. MacDonald, Phys. Rev. Lett. **67**, 2060 (1991); A. H. MacDonald, S. R. Eric Yang, and M. D. Johnson, Aust. J. Phys **46**, 345 (1993).
 [7] Y. Meir, Phys. Rev. Lett. **72**, 2624 (1994).
 [8] C. L. Kane, Matthew P. A. Fisher, and J. Polchinski, Phys. Rev. Lett. **72**, 4129 (1994).
 [9] C. L. Kane and Matthew P. A. Fisher, Phys. Rev. Lett. **76**, 3192 (1996).
 [10] O. Klein, C. de C. Chamon, D. Tang, D. M. Abusch-Magder, U. Meirav, X.-G. Wen, M. A. Kastner, and S. J. Wind, Phys. Rev. Lett. **74**, 785 (1995).
 [11] N. B. Zhitenev, M. Brodsky, R. C. Ashoori, and M. R. Melloch, Phys. Rev. Lett. **77**, 1833 (1996).
 [12] V. Venkatachalam, S. Hart, L. Pfeiffer, K. West, and A. Yacoby, Nature Phys. **8**, 676 (2012).
 [13] A. Grivnin, H. Inoue, Y. Ronen, Y. Baum, M. Heiblum, V. Umansky, and D. Mahalu, Phys. Rev. Lett. **113**, 266803 (2014).
 [14] R. Sabo, I. Gurman, A. Rosenblatt, F. Lafont, D. Banitt, J. Park, M. Heiblum, Y. Gefen, V. Umansky, and D. Mahalu, Nature Phys. **13**, 491 (2017).
 [15] X. Wan, K. Yang, and E. H. Rezayi, Phys. Rev. Lett. **88**, 056802 (2002).
 [16] K. Yang, Phys. Rev. Lett. **91**, 036802 (2003).
 [17] Y. Zhang, Z.-X. Hu, and K. Yang, Phys. Rev. B **88**, 205128 (2013).
 [18] Y. Barlas, Y. N. Joglekar, and K. Yang, Phys. Rev. B **83**, 205307 (2011).
 [19] Y. Zhang and K. Yang, Phys. Rev. B **87**, 125140 (2013).
 [20] J. Wang, Y. Meir, and Y. Gefen, Phys. Rev. Lett. **111**, 246803 (2013).
 [21] J. Wang, Y. Meir, and Y. Gefen, Phys. Rev. Lett. **118**, 046801 (2017).
 [22] Coulomb interactions have both direct and exchange components, so there can be confusion about what is meant by “charge” versus “exchange” effects. Our working definition is that when a reorganization of the charge density occurs as a consequence of a edge reconstruction it is essentially a “charge” effect, while any reconstruction without such a reorganization of charge density is essentially an “exchange” effect.
 [23] R. E. Prange and S. M. Girvin, The Quantum Hall Effect, Springer-Verlag New York (1990).
 [24] T. Jungwirth and A. H. MacDonald, Phys. Rev. B **63**, 035305 (2000).
 [25] J. T. Chalker, D. G. Polyakov, F. Evers, A. D. Mirlin, and P. Wolffe, Phys. Rev. B **66**, 161317(R) (2002).
 [26] E. H. Rezayi, T. Jungwirth, A. H. MacDonald, and F. D. M. Haldane, Phys. Rev. B **67**, 201305 (2003).
 [27] Further details are presented in the Supplemental Material.
 [28] Our work so far has focused on translation invariant states along the edge. In the situations we consider for experimental signatures, the slope of V_{edge} changes along the edge. We assume that as long as the changes occur over a scale long compared to ℓ our analysis remains valid. We also assume that in this region, there is a mechanism which allows the spin to relax to its equilibrium value.
 [29] D. G. Polyakov, Phys. Rev. B **53**, 15777 (1996).
 [30] D. I. Golosov, I. Shlimak, A. Butenko, K.-J. Friedland, and S. V. Kravchenko, Phys. Rev. B **88**, 155313 (2013).
 [31] S. L. Sondhi, A. Karlhede, S. A. Kivelson, and E. H. Rezayi, Phys. Rev. B **47**, 16419 (1993).
 [32] J. K. Jain and X. G. Wu, Phys. Rev. B **49**, 5085(R) (1994).
 [33] X. G. Wu and S. L. Sondhi, Phys. Rev. B **51**, 14725 (1995).
 [34] A. Karlhede, S. A. Kivelson, K. Lejnell, and S. L. Sondhi, Phys. Rev. Lett. **77**, 2061 (1996).
 [35] D. A. Abanin, S. A. Parameswaran, and S. L. Sondhi, Phys. Rev. Lett. **103**, 076802 (2009).
 [36] D. A. Abanin, P. A. Lee, and L. S. Levitov, Phys. Rev. Lett. **96**, 176803 (2006).
 [37] L. Brey and H. A. Fertig, Phys. Rev. B **73**, 195408 (2006).
 [38] H. A. Fertig and L. Brey, Phys. Rev. Lett. **97**, 116805 (2006).
 [39] J. K. Jain, Phys. Rev. Lett. **63**, 199 (1989); Phys. Rev. B **41**, 7653 (1990); *Science* **266**, 1199 (1994).